Energy Reports 6 (2020) 238–253

Contents lists available at ScienceDirect

Energy Reports

journal homepage: www.elsevier.com/locate/egyr

Research Paper

Thermal analysis of a portable DSSC mini greenhouse for botanical drugs cultivation

L. Lu [a,e], M.E. Ya'acob [b,c,*], M.S. Anuar [b], G. Chen [d], M.H. Othman [e], A. Noor Iskandar [b,e], N. Roslan [b,e]

[a] Department of Electrical and Electronics Engineering, Faculty of Engineering, Universiti Putra Malaysia, Serdang, 43400, Selangor, Malaysia
[b] Department of Process and Food Engineering, Faculty of Engineering, Universiti Putra Malaysia, Serdang, 43400, Selangor, Malaysia
[c] Centre for Advanced Lightning, Power and Energy Research (ALPER), Universiti Putra Malaysia, Serdang, 43400, Selangor, Malaysia
[d] Faculty of Health, Engineering and Sciences, University of Southern Queensland, Toowoomba, QLD, 4350, Australia
[e] Hybrid Agrivoltaic Systems Showcase (HAVs) eDU-PARK, Universiti Putra Malaysia, Serdang, 43400, Selangor, Malaysia

ARTICLE INFO

Article history:
Received 18 October 2019
Received in revised form 18 December 2019
Accepted 29 December 2019
Available online xxxx

Keywords:
Mini greenhouse
Shading mechanism
DSSC
Botanical drugs
Thermal analysis

ABSTRACT

Photovoltaic farms in Malaysia are being developed tremendously as a form of supporting fossil fuel setbacks in Malaysia power generation. An important parameter of the PV installation is the power (Watts) accumulated over sunlight retrieval. Considerable losses may arise from the conversion, where the efficiency is typically 15% to 23%, with the remainder becoming losses in the form of accumulated heat under the PV array or panel installations. PV heat dissipation is dependent on solar radiation, air convection and PV cell conduction. Dye Sensitized Solar Cell (DSSC) has been applied as a greenhouse shading element, having the ability of enabling specified spectrum of light color penetration during electric accumulation. Furthermore, only light of wavelength between 400 and 700 nm (PAR) is absorbed by the greenhouse plants which is essential for their growth and photosynthesis. A Portable DSSC Mini Greenhouse (PDMG) can provide simple, effective and suitable light source for botanical drugs. Light which is associated with increasing temperature and heat is critical to be measured. A measurement of average heat gain flowing into a building through building envelope (OTTV- Overall Thermal Transfer Value) is a well-known method adopted in green building design. In this paper, the OTTV approach is applied to calculate heat transfer properties, from outdoor surroundings to the PDMG structure, giving justification of the PDMG thermal conditions.

1. Introduction

In energy efficiency strategies and plans, a building code or standard is essential where each building is defined to provide energy proficiency in the areas of material, structure, facility and system. Heat gain needs to be taken in consideration as careful management of this effect can enable significant energy savings. The same method is being used in providing thermal comfort in the building, while enabling managers to trim cost on building management (Djamila et al., 2018).

Environment temperature is highly dependent on surrounding and geographical area, and is affected by seasonal changes on the atmospheric precipitation and flow based on sea and land temperature (Chan and Chow, 2013). In order to reduce external heat gain into a building, the concept of OTTV is developed and adopted in many countries, especially some Asian countries or regions with fully air-conditioned climates (Devgan et al., 2010). Singapore was the first Asian country to adopt an OTTV standard, modified from the American Society of Heating, Refrigerating and Air-conditioning Engineers (ASHRAE) Standards 90–75 and 90–80A in 1979 and hence effectively minimize the cooling load of the air-conditioned buildings or systems. Later on, some other Asian countries including Thailand, Malaysia and Indonesia also developed OTTV standards in 1980s and 1990s to suit their local climates and construction methods (Oraee and Luther, 2015). In 1995, the Hong Kong government proposed that an OTTV control measure was used for designing in commercial buildings (Chan, 2019; Jia and Lee, 2018).

The OTTV, which estimates the average rate of heat transfer into the building through its envelope, acts as a thermal performance index (Hwang et al., 2018). An OTTV calculation is highly dependent upon the location, e.g. Malaysia, where temperature data is suited to the area of work. Manual based OTTV, needs considerations of multiple functions based on multiple coefficients and variables, internal and external (Natephra et al., 2018). Many

* Corresponding author at: Department of Process and Food Engineering, Faculty of Engineering, Universiti Putra Malaysia, Serdang, 43400, Selangor, Malaysia.
E-mail address: fendyupm@gmail.com (M.E. Ya'acob).

https://doi.org/10.1016/j.egyr.2019.12.025

Glossary

ETTV	Envelope Thermal Transfer Value (Wm^{-2})
$OTTV_w$	Overall Thermal Transfer Value for wall (Wm^{-2})
$OTTV_r$	Overall Thermal Transfer Value for roof (Wm^{-2})
RTTV	Roof Thermal Transfer Value (Wm^{-2})
R-value	Thermal Resistance (m^2KW^{-1})
U-value	Thermal Transmittance ($Wm^{-2}K^{-1}$)

Nomenclature

A_w, A_f	opaque wall area and fenestration wall area (m^2)
A_{ow}	gross area of walls where $A_{ow} = A_w + A_f$ (m^2)
A_r, A_s, Af_r	opaque roof area, skylight area and fenestration roof area (m^2)
A_{or}	gross area of roof where $A_{or} = A_r + A_s$ or $A_{or} = A_r + Af_r$ (m^2)
CF	solar correction factor for fenestration (use in Singapore)
ESM	external shading multiplier (for solar shading device)
ESR	effective solar radiation (Wm^{-2})
OF	solar orientation factor (use in Malaysia), which is the same with CF
SC	shading coefficient
SF	solar factor for fenestration (Wm^{-2})
$SHGC$	solar heat gain coefficient
SKR, SRR	ratio between skylight area and gross area of roof where $SKR = A_s/A_{or}$
TD_{eq}	equivalent temperature difference (K)
TD_{EQw}, TD_{EQr}	equivalent temperature difference for wall and roof (K)
ΔT	temperature difference between external and internal design conditions (K)
U_w, U_f	thermal transmittance of opaque wall and fenestration wall ($Wm^{-2}K^{-1}$)
U_r, $U_{op-roof}$	thermal transmittance of opaque roof ($Wm^{-2}K^{-1}$)
U_s, $U_{skylight}$	thermal transmittance of skylight roof ($Wm^{-2}K^{-1}$)
WWR	window-to-external wall ratio where $WWR = A_f/A_{ow}$
α	solar absorptivity, which is related with the color of walls
α_w, α_r	solar absorptivity of opaque wall and opaque roof

studies on OTTV were carried out by researchers from all over the world. In Malaysia, Harun et al. (2017) reported that green building was environmental-friendly to the surrounding, it used less electricity and had lower OTTV. A Genetic Algorithm (GA) was also used for optimizing green building designed by Building Information Modelling (BIM) software. The aim was to find an optimum combination of materials, so that an optimum OTTV was produced. The research result showed that GA was able to reduce 16% of OTTV by finding optimum combinations of materials. In Japan, a similar work was proposed by Natephra et al. (2018). Through a BIM-based method, data was extracted from BIM database to calculate OTTV of building envelope by using a visual programming interface, then energy-efficient design of the buildings was achieved.

Dye-sensitized solar cells (DSSC), which was originally co-created by Michael Grätzel and Brian O'Regan in 1988, is known as Grätzel cells (Sharma et al., 2018). DSSC is an electrochemical device that generates electricity from the sunlight by using dye-sensitized method on semiconductors. The DSSC module basically has five components: dye as photosensitizer, electrolytes, conductive glass or substrates, photo-electrode and counter electrode. One of the most important elements of DSSC is photosensitizer. This is because dye has a significant effect on the efficiency of absorbing and converting solar energy to electricity. Hence, best selection of dye in DSSC can achieve the great efficiency (Kane et al., 2016; Adedokun et al., 2016; Hussein et al., 2018). As the third generation of PV technology, DSSC currently has the potential to serve as an ideal material in different types of applications, including mini greenhouse systems. This is because that DSSC possesses many outstanding features, including low-cost fabrication, good conversion-efficiency and low-sensitive to light level. Besides, it also has beneficial features on low material usage and flexible scale. Obviously, these characteristics allow DSSC to play an important role in energy-saving buildings (Roslan et al., 2018; Iwata et al., 2018).

Greenhouse is a breakthrough technology that is widely used in the agriculture and cultivation since it provides two main benefits. The greenhouse creates a favorable microclimate environment against outside harsh environmental conditions such as extreme temperature, rain and wind for greater crop quality and productivity (Ezzaeri et al., 2018; Ghani et al., 2019). The other benefit is that greenhouse offers out-of-season cultivation (Taki et al., 2018). The greenhouses are normally built on open areas with enough sunlight because sunshine is an essential demand for crop photosynthesis. The walls and roofs of greenhouse are composed of transparent plastic or glass (Yano and Cossu, 2019). Then a common problem of normal greenhouses has emerged: low temperature during winter or overheating during summer because of the solar radiation and seasonal air temperature. To solve this problem, PV panels (as sunshade device) integrated greenhouse have been developed which are simultaneously used for plant photosynthesis and electricity production (Gao et al., 2019). However, covering ratio of PV in the greenhouse becomes a primary concern. Otherwise, productions of shade-intolerant plants are reduced due to PV shading effect. Then semi-transparent PV panels integrated greenhouse have been developed (Cossu et al., 2018). Fig. 1 shows the revolution of PV greenhouses, which is from conventional PV greenhouses (opaque) to semi-transparent DSSC greenhouse.

The current OTTV calculation method was mainly used for conventional buildings with concrete, transparent glass windows etc. With the increasing awareness of environmental protection in recent years, PV system is also being widely used in the building applications because of the two benefits. It can generate electricity through the solar energy and reduce the heat gain transmitted into the building envelope. Chan (2018) presented three buildings with PV glazing system in Hong Kong of China. The result of this case study revealed that PV glazing system led to significant reduction in heat gain. Hence, incorporating the effect of PV glazing system into the OTTV regulation was recommended. Besides, based on the research on OTTV regulation in Hong Kong, it is obvious that the methodology can also be applied to other countries with different climatic conditions e.g. Singapore.

Why is it necessary for greenhouse to define OTTV? Botanical drugs consist of natural substances which have constituents

Fig. 1. Revolution of PV greenhouse (a) crystalline silicon modules greenhouse (Castellano et al., 2016), (b) thin film amorphous modules greenhouse (Hassanien et al., 2016) and (c) semi-transparent DSSC greenhouse.

with medicinal activities or heath-enhancing. Therefore, botanical drugs are also called as natural drugs (Ahn, 2017). Botanical drugs have not only a decisive function in drug discovery but also in boosting national economic growth. Therefore, it is meaningful question that greenhouse whether can provide a suitable growing environment for botanical drugs or not. The light for entering the greenhouse is a significant factor. Different kinds of plants e.g. botanical drugs have their own light requirements. Most of plants in the greenhouse grow best when the light wavelength band lies between 400 and 700 nm (PAR). So too much light can cause heat stress to plants (Lamnatou and Chemisana, 2013). During summer season excessive temperature then can cause a detrimental effect on plants yield especially in tropical regions (Kumar et al., 2009). Taking Malaysia from Southeast Asian countries as an example, the temperature is approximately 26 °C–35 °C all around the year. Heat stress to plants in the greenhouse is a practical issue. As a thermal performance index, OTTV can estimate the total heat gain transmit through outer layer of greenhouse to reasonably provide the reasons that which part construction of greenhouse absorbs much more heat and directly causes the heat stress to plants inside the greenhouse. In the end, heat stress to plants would be solved accordingly based on OTTV evaluation. Besides, it would also help to reduce energy consumption from cooling system in some greenhouses indirectly.

Recently, there have been few research papers with respect to OTTV calculations on the greenhouse, especially OTTV calculations on the PV integrated greenhouse e.g. DSSC installed as the roof of greenhouse, so there is also no OTTV standard values for PV greenhouse. In addition, most paper were mainly focused on OTTV calculations for the walls of buildings in Asian tropical regions. Particularly, current design parameter of OTTV calculation have not included the heat energy absorbed by the building envelope from the roof. This paper therefore applies OTTV approach to calculate heat transfer properties for both the walls and DSSC roof of PDMG system, giving justification of the PDMG thermal conditions.

1.1. Different OTTV calculations in Asia

A lot of OTTV calculations are available throughout the world, particularly in the Asian countries. ASHRAE Standard 90–75 provides first development of OTTV, requiring that 50 W/m^2 should not exceeded. Variations of OTTV calculations are high as OTTV is subjected to the influence of the place where system or building is located. Malaysia, Singapore, Thailand and Hong Kong have thus developed their own standards of OTTV assessment. Taking tropical countries Malaysia, Singapore and Thailand as examples, OTTV calculations for the walls comprise three main ways of heat transfer through the outermost layer of a given building: (i) heat conduction transmitted through the opaque walls, (ii) heat conduction transmitted through glass windows, and (iii) solar radiation transmitted through window glass (Singhpoo et al., 2015; Seghier et al., 2017; Consumption, 2009). The roof OTTV calculations also consist of three main elements: (i) heat conduction through the roof's opaque portion, (ii) heat conduction through the roof's skylight portion and (iii) solar radiation through the roof's skylight portion (Energy efficiency and use of renewable energy for non-residential buildings, 2014). It is noted that the components in the following presented OTTV equations about the walls and roofs respectively are shown in same sequence as above.

Eq. (1) was the initial form of OTTV calculation for walls in Malaysia (Anon, 1992). Then the modified OTTV calculations for Malaysia reference on OTTV can be traced from Malaysia Standard MS1525:2014. It recommended that the OTTV of the building envelope (excluding the roof) for a building with a total air-conditioned area exceeding 1000 m^2 should not be more than 50 W/m^2. The following parameters $TD_{eq} = 15K$, $\Delta T = 6$ K and $SF = 194$ W/m^2 were set for developing the calculation of OTTV for walls, which is shown in Eq. (2) (Energy efficiency and use of renewable energy for non-residential buildings, 2014).

$$OTTV_w = TD_{eq}(\alpha)(1 - WWR)(U_w) + \Delta T(WWR)(U_f) + SF(WWR)(OF)(SC) \quad (1)$$

$$= 15\alpha \times (1 - WWR) \times U_w + 6 \times WWR \times U_f + 194 \times WWR \times OF \times SC \quad (2)$$

The OTTV formula for roof with skylights in Malaysia as shown in Eq. (3), and the maximum recommended OTTV for roofs with skylight is 25 W/m^2 (Energy efficiency and use of renewable energy for non-residential buildings, 2014). Based on the definition of SKR, Eq. (3) can be simplified as Eq. (4).

$$OTTV_r = \frac{(A_r \times U_r \times TD_{eq}) + (A_s \times U_s \times \Delta T) + (A_s \times SC \times SF)}{A_{or}} \quad (3)$$

$$= TD_{eq} \times (1 - SKR) \times U_r + \Delta T \times SKR \times U_s + SF \times SKR \times SC \quad (4)$$

The ETTV model is currently adopted in Singapore, which is similar with the concept of walls' OTTV. It is also developed for indicating solar heat gain transmitted into the building envelope excluding the roof. Eq. (5) shows the initial form of ETTV model for walls. Based on multi-parametric simulations, the following values: $TD_{eq} = 12$ K, $\Delta T = 3.4$ K and $SF = 211$ W/m^2 at $T_c = 25$ °C were used for developing the ETTV calculation. Under Singapore's context, the calculation of ETTV is expressed as Eq. (6) (Chua and Chou, 2010, 2011). The maximum value of ETTV for non-residential buildings was also set at 50 W/m^2 by Singapore Building Codes Authority in 2008, when air-conditioned area exceeds 500 m^2 (Natephra et al., 2018).

$$ETTV = TD_{eq} \times (1 - WWR) \times U_w + \Delta T \times WWR \times U_f + SF \times WWR \times CF \times SC \quad (5)$$

$$= 12 \times (1 - WWR) \times U_w + 3.4 \times WWR \times U_f + 211 \times WWR \times CF \times SC \quad (6)$$

The general RTTV model of roof calculation for Singapore is given by Eq. (7). Then the updated calculation of RTTV for Singapore is expressed as Eq. (8) by using TD_{eq}(12.5 K), ΔT(4.8 K) and SF(485 W/m^2) (Zingre et al., 2015). The maximum allowable RTTV for commercial buildings is 50 W/m^2 with air-conditioned area more than 500 m^2 (Natephra et al., 2018).

$$RTTV = TD_{eq}\,(1 - SKR)\,U_{op-roof} + \Delta T\,(SKR)\,U_{skylight} + SF(SKR)(CF)(SC) \quad (7)$$

$$= 12.5\,(1 - SKR)\,U_{op-roof} + 4.8\,(SKR)\,U_{skylight} + 485(SKR)(CF)(SC) \quad (8)$$

The OTTV equation for walls of buildings in Thailand is expressed as Eq. (9). OTTV values should not exceed 50 W/m^2 for school and office buildings, and 40 W/m^2 for hypermarket and 30 W/m^2 for hotels and hospitals when air-conditioned area is no less than 2000 m^2 (Chirarattananon et al., 2010).

$$OTTV_w = TD_{eq} \times (1 - WWR) \times U_w + \Delta T \times WWR \times U_f + WWR \times SHGC \times ESR \times SC \quad (9)$$

The OTTV calculation for the roof in Thailand is expressed as Eq. (10) (Natephra et al., 2018). For the same type of buildings like above, the uppermost roof OTTV values were set at 15 W/m^2, 12 W/m^2 and 10 W/m^2 when air-conditioned area exceeds 2000 m^2 (Chirarattananon et al., 2010).

$$OTTV_r = \left(TD_{eq}\right)(1 - SRR)\,(U_r) + (\Delta T)\,(SRR)\,(U_s) + (SRR)(SHGC)(ESR)(SC) \quad (10)$$

As a subtropical city of China, elements for OTTV walls and roof calculations respectively in Hong Kong are different with above three countries. The OTTV model in Hong Kong has only two main components: (i) heat conduction through opaque walls and (ii) solar radiation through glass windows. This is because heat conduction through glass windows had little effect when compared to above two components. The maximum values of average heat transfer through a given building tower envelope and podium are set as 24 Wm^{-2} and 56 Wm^{-2} respectively (Chan and Chow, 2014). The formula of OTTV for wall in Hong Kong as shown in Eq. (11) (Wong and Chan, 2012). Based on the definition of WWR, the modified equation as shown in (12).

$$OTTV_w = \frac{\left(TD_{EQ\,w} \times \alpha_w \times A_w \times U_w\right) + (A_f \times SC \times ESM \times SF)}{A_{ow}} \quad (11)$$

$$= TD_{EQ\,w} \times \alpha_w \times (1 - WWR) \times U_w + SF \times WWR \times ESM \times SC \quad (12)$$

The OTTV calculation of roof in Hong Kong also consists of two parts: (i) heat conduction through opaque portion of roof and (ii) solar radiation through skylight portion of roof. Eq. (13) shows OTTV calculation for roof in Hong Kong. The upper limit of roof OTTV has the same requirement as OTTV of walls (Anon, 1995). The modified equation as shown in (14).

$$OTTV_r = \frac{(A_r \times U_r \times \alpha_r \times TD_{EQr}) + (Af_r \times SC \times SF)}{A_{or}} \quad (13)$$

$$= TD_{EQr} \times \alpha_r \times (1 - SKR) \times U_r + SF \times SKR \times SC \quad (14)$$

Based on above equations, Table 1 shows and compares the parameters of OTTV calculations for wall and roof used in Malaysia, Singapore, Thailand and Hong Kong of China. In the Table, checks mean that parameters are used in the OTTV calculation and crosses state that parameters are not used in the OTTV calculation. And the blank represents that the component is not considered in the OTTV calculation i.e. In Hong Kong, heat conduction through window glass in the OTTV calculation for the wall and heat conduction through skylight portion of roof in the OTTV calculation for the roof are neglected respectively due to insignificant effect, which is stated above.

For OTTV calculation of wall, four parameters TD_{eq}, α, $(1 - WWR)$ and U_w for heat conduction through opaque walls are all considered in some countries or region, but solar absorptivity α is not taken into account in heat conduction calculation through opaque walls in Singapore and Thailand. Solar absorptivity α is related with the color of wall. It is known that black color can absorb more heat than other colors. For instance, solar absorptivity of black concrete (0.91) is higher than that of brown concrete (0.85), so heat transfer is higher for darker color of concrete (Wong and Chan, 2012). As a result, heat conduction calculation through opaque walls can be affected by neglecting solar absorptivity. For OTTV calculation of roof in heat conduction through opaque portion of roof, the cons of neglecting solar absorptivity for three countries is similar with walls'.

Three countries all take into account three parameters ΔT, WWR and U_f of walls in heat conduction calculation through window glass. WWR and SKR or SRR (for roof) is an important parameter, which affects the overall thermal transfer through walls in various directions. For example, normally large value of WWR or SKR indicates that a large amount of energy would be used for cooling the space (Natephra et al., 2018).

For solar radiation through window glass of walls, shading coefficient SC and WWR are both considered in all countries or region. The related explanation in terms of SC is discussed in Section 2.2. However, solar factor SF, which is the hourly radiation per square meter for vertical and horizontal surfaces, is only omitted in Thailand. It can be seen from fixed values in Malaysia (194 Wm^{-2}) and Singapore (211 Wm^{-2}) that solar factor has an effect on the solar radiation calculation through window glass. Besides, solar orientation factor OF or solar correction factor CF for wall is also neglected by Thailand and Hong Kong. This coefficient should be considered because different orientations of all walls has different solar orientation factors. For solar radiation through skylight portion of roof, explanation for related parameters of skylight roof is similar with above mentioned parameters of walls.

Moreover, the parameters TD_{eq}, ΔT and SF for walls in Malaysia and Singapore are fixed value. It may cause the limitation because these values are varied with the local weather all the time. For OTTV calculation of roof, same parameters are also fixed in Singapore. The thermal transmittance U-value, which is taken into account for wall and roof in all countries or region, is also an essential coefficient. The related explanation in terms of thermal transmittance is discussed in Section 2.1.

According to above different OTTV equations, it is necessary to control the OTTV and thus the amount of heat transfer through buildings' envelope during the building design process. The higher OTTV is, the more heat gain absorbed by the building (Vijayalaxmi, 2010). This leads to a rapid increase in the internal temperature of buildings. Hence, the consumption of building electricity would be significantly increased due to highly frequent usage of air conditioner. Meanwhile, it also increases the greenhouse gas emissions (Harun et al., 2017).

1.2. Market demand for botanical drugs

OTTV is critical for greenhouse because heat stress to plants e.g. botanical drugs in the greenhouse is a practical issue. It can provide the suitable growth environment for botanical drugs based on the heat justification for the greenhouse.

Based on the World Health Organization (WHO), there are around 80% of the population in developing countries relying on

Table 1
Comparison of the parameters used in Malaysia, Singapore, Thailand and Hong Kong of China.

Wall	Malaysia	Singapore	Thailand	Hong Kong, China
	Heat conduction through opaque walls			
TD_{eq} or $TD_{EQ,w}$	15	12	✔	✔
α or α_w	✔	✗	✗	✔
$(1-WWR)$	✔	✔	✔	✔
U_w	✔	✔	✔	✔
	Heat conduction through window glass			
ΔT	6	3.4	✔	
WWR	✔	✔	✔	
U_f	✔	✔	✔	
	Solar radiation through window glass			
SF	194	211	✗	✔
WWR	✔	✔	✔	✔
OF or CF	✔	✔	✗	✗
SHGC	✗	✗	✔	✗
ESR	✗	✗	✔	✗
ESM	✗	✗	✗	✔
SC	✔	✔	✔	✔
Roof	Malaysia	Singapore	Thailand	Hong Kong, China
	Heat conduction through opaque portion of roof			
TD_{eq} or TD_{EQr}	✔	12.5	✔	✔
α_r	✗	✗	✗	✔
$(1-$ SKR$)$ or $(1-$ SRR$)$	✔	✔	✔	✔
U_r or $U_{op-roof}$	✔	✔	✔	✔
	Heat conduction through skylight portion of roof			
ΔT	✔	4.8	✔	
SKR or SRR	✔	✔	✔	
U_s or $U_{skylight}$	✔	✔	✔	
	Solar radiation through skylight portion of roof			
SF	✔	485	✗	✔
SKR or SRR	✔	✔	✔	✔
CF	✗	✔	✗	✗
SHGC	✗	✗	✔	✗
ESR	✗	✗	✔	✗
SC	✔	✔	✔	✔

medical plant preparations to meet their basic needs on health care (Kakooza-mwesige, 2015). Nowadays, botanical medicines are of great importance in the global market due to some noticeable factors. For example, synthetic drugs can not only cause extremely unpleasant side-effects including weight gain, allergy and acne but also high cost. Furthermore, the prevalence of chronic diseases keeps on increasing and botanical drugs are low-cost. Besides, botanical drugs are important component of traditional medicines e.g. homeopathy and Ayurveda (Botanical and Plant Derived Drugs Market, 2019). The global market value of botanical medicines reached at US $72 billion in 2016, and the global market is estimated that will steadily grow to more than US $111 billion by 2023 (Upton et al., 2019). This rapidly growing global market states that botanical drugs have played and will continue to play an extremely significant role in drug discovery for human's health care in the forthcoming years. Fig. 2 shows the tendency of botanical and plant-derived drugs market in Asia Pacific from 2016 to 2026, and it is obvious that all countries have a growing trend especially China. The market size accounted for $15954 million in 2017 (Anon, 2017a). In Europe, the market of botanical and plant-derived drugs generated the revenue of $5144 million in 2017 and it can reach at $9820 million by the end of 2018–2016 (Anon, 2017b). The market for North America was valued to be at $3804 million on botanical and plant-derived drugs in 2017, then it can generate around $7032 million from 2018 to 2026 (Anon, 2017c). Therefore, it is clear that the market demand for botanical drugs is considerable.

Botanical drugs typically contain heterogeneous compositions that originates from herbal practices, and clinically validated pharmaceuticals of plant origin can also be simply defined for botanical drugs. Based on US Food and Drug Administration (FDA), the botanical drugs contain ingredients that come from plant parts, isolated or combined chemical components of plant origin, dried or fresh plants, macroscopic fungi, algae, or combinations thereof. Botanical drugs can be available in various types of forms such as pills, tablets, injections and capsules. They can be used in the treatment of many health conditions in humans such as respiratory diseases, infectious diseases and cardiovascular diseases (Liu and Wang, 2008).

In Malaysia, the Gross National Income (GNI) was significantly affected because the global market value on the traditional agricultural commodity e.g. rubber, palm oil was on a downward trend. In order to boost national economic growth for agricultural components as shown in Fig. 3, so Malaysia government illustrated some strategic focuses on the Economic Transformation Program (ETP). Through large funds initiatives, this effort also contributes to productivity gains in stimulating the economy (Othman et al., 2015). The ETP/Entry Point Project 1 (EPP1) contributed RM7.4 billion to the GNI in 2013, this helped to create 29,373 new employment opportunities and drive RM8 billion worth of investments (Othman et al., 2016). Based on the economic transformation program, the Agriculture National Key Economic Area (NKEA) has three main aspirations:

(i) Increasing GNI contribution by RM28.9 billion, to reach RM49.1 billion in 2020, more than double the current size of the sector.
(ii) Creating 74,600 job opportunities, the bulk of which will be in rural areas.
(iii) Increasing the incomes of farmers participating in NKEA initiatives by two to four times.

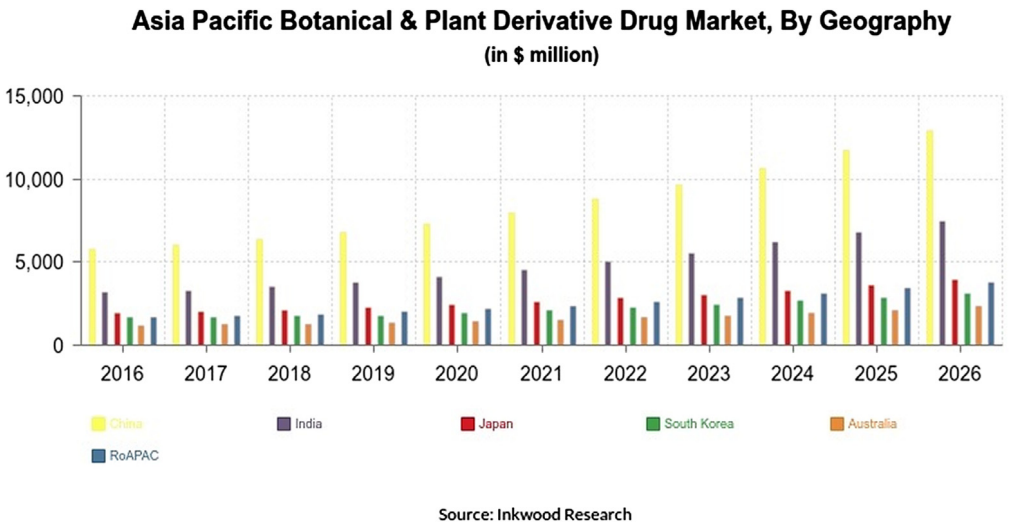

Fig. 2. Botanical & Plant Derivative Drug Market in Asia Pacific.
Source: From Anon (2017a).

Fig. 3. National initiatives to boost herbal products towards agri-business.
Source: From http://www.moa.gov.my.

These targets will involve capturing higher value production and increasing productivity. Downstream investment in higher-value activities will be catalyzed for edible bird's nest, herbal products and processed food respectively.

Herbal products can be extracted as the botanical drugs because of good potential and high value bioactive compounds. As a result, this drug class often has unique features such as complex mixtures and a lack of distinct bioactive components (Goldman, 2001). Clinical Studies reviewed by Othman et al. (2016), Yang and Song (2014), Moreira et al. (2013), Zanoli et al. (2009) and Mohamed et al. (2013) have shown great potential of the herbal compounds as botanical drugs in treating diseases including cancer and therefore a suitable greenhouse with light spectrum treatment are proposed.

1.3. Light spectrum via DSSC

Most of the prior art technologies is related to silicon-based Photovoltaic (PV) integrated greenhouse. The most prominent problem manifested by silicon-based PV is opaque to sunlight and it will cause irreconcilable competition between PV roofs and plants. Thus, in such conditions, reduction of Photosynthetically Active Radiation (PAR) will give adverse effect especially to the crops and plants inside the greenhouse (Marcelis and Broekhuijsen, 2006; Schettini et al., 2011).

Fig. 4 shows the solar spectrum with emphasis on the PAR wavelength. The main picture in Fig. 4 illustrates 51% in the infrared range IR, 43% in the visible spectrum (400–700 nm) and remaining 6% in the ultraviolet UV (300–400 nm) at the surface of Earth. The black curve stands for solar energy that reaches the earth surface Air Mass 1.5 (AM 1.5). It means that spectral filtering through 1.5 depth of cloudless atmosphere, delivering a maximum irradiance value of 1000 Wm^{-2}. The white curve, which represents solar spectrum distribution at the top of atmosphere, is named as the Air Mass (AM 0) spectrum. The sub picture in Fig. 4 illustrates that the wavelength of solar spectrum between 400 and 700 nm is designated as PAR, which is typically essential in photosynthesis process of plant cultivation. Chlorophyll is the most abundant plant is most efficient in capturing red (660 nm) and blue (440 nm) light which absorbed by chlorophyll a & chlorophyll b respectively (Roslan et al., 2018; Ringsmuth et al., 2016). The photosynthesis is related with the red spectrum band and the blue band corresponds to the photomorphogenic and phototropic responses of plants (Kim et al., 2014).

It is generally known that light has long been accepted as an essential and vital element in plant growth (Hammam et al., 2007). As mentioned in Section 1, DSSC is sensitive to low light level. Therefore, in order to improve the quality and quantity of plants' products, it is very important to do the preparation of DSSC for greenhouse in light manipulation (Kim et al., 2014). The various color of DSSC (determined by the dye) can act as plant growth regulator or photoselective shading in order to modify the light spectrum which enters the greenhouse. Previous research by Kadowaki et al. (2012) for Welsh growth onion, Marrou et al. (2013) for lettuces and Schettini et al. (2011) for peach and cherry tree growth have shown significant findings of shading effects on greenhouse conditions. Marcelis and Broekhuijsen (2006) claims that 1% drop in plants' photosynthesis would result in significantly reflect 1% reduction in the crop production, it is mainly for the case of greenhouse plants e.g. vegetables and flowers.

2. Heat dissipation via DSSC materials

Normal silicon-based photovoltaic panels are used for directly converting solar irradiation into electricity (Rahman et al., 2015). However, generally only about 15%–23% of the solar energy can be converted to electrical energy (Abdelrazik et al., 2018; NREL

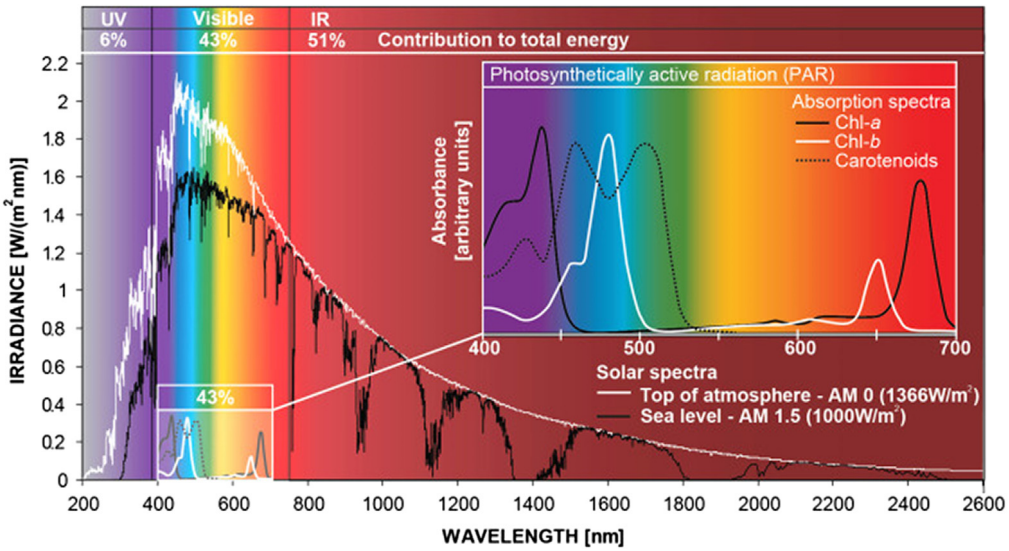

Fig. 4. PAR spectrum in sun irradiance. . (For interpretation of the references to color in this figure legend, the reader is referred to the web version of this article.) *Source:* From Roslan et al. (2018).

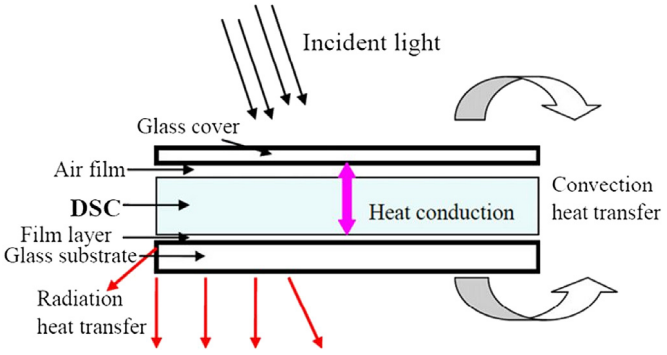

Fig. 5. The thermal model of DSSC module.

Transforming ENERGY, 2018). The remaining portion of the solar energy is developed into the heat loss (Du et al., 2017), which increases the temperature of panels. This temperature rise decreases the PV module efficiency and also leads to the thermal stress in the panels (Siddiqui and Arif, 2013). Therefore, good heat dissipation facilitates high efficiency of PV solar cell. The power conversion efficiencies (PCEs) of DSSCs have maintained in the range between 11% and 12% for many years. However, the PCE of solid-state DSSC have been reported over 14% (around 15%) with small-active area in 2013 (Skandalos and Karamanis, 2015; Selvaraj et al., 2018).

Heat dissipation is one type of heat transfer. It occurs when an object is hotter than other objectives in an environment. It means that the colder objects or the surrounding environment are transferred by the heat of the hotter object. There are also three main heat dissipation occurring from PV modules: (i) heat dissipation by conduction (ii) heat dissipation by convection (iii) heat dissipation by radiation (Kim et al., 2016). Fig. 5, taking DSSC module as an example, shows the three main paths of heat dissipation.

The conductive heat dissipation occurs when there are thermal gradients between DSSC module and other materials, these materials are in physical contact with the DSSC module. So, when the heat flux is transmitted across an interface between the module surface and the DSSC, then a finite temperature discontinuity at the interface will be caused by the interfacial thermal resistance. It is fundamental that the thermal resistance and the configuration of the materials used in the DSSC module have the ability to transfer heat from DSSC module to its surroundings. Moreover, the thermal resistance of DSSC module is characterized by the thickness and the thermal conductivity of the material. This means that the use of different materials in the DSSC modules has a major impact on the heat dissipation by conduction.

The convective heat loss is caused by the fluid motion, which occurs between an object and its environment. In DSSC module, the generated heat is dissipated by the convection through the front and back-side of DSSC module because of wind blowing across the module surface. The final way is heat dissipation by radiation, which transfers heat to the surrounding environment. Because of radiation, the net heat lost from the module is the difference between the heat radiated from the surroundings to the DSSC module and the heat radiated from the DSSC module to the surroundings (Chen et al., 2013; Khanna et al., 2017).

2.1. Thermal transmittance (U-value) of materials

The thermal transmittance of a material, such as concrete or insulation, is presented as a U-value. In order to achieve the desirable energy performance in building construction, a lower U-value is preferred. In other words, a higher U-values indicates the worse thermal insulation performance of building components (Cuce, 2018). Hence, using an inadequate U-value will contribute to unnecessary or costly energy conservation methods to be applied in the building (Fernandes et al., 2019). To calculate the U-value of elements used in the building, two parameters are required to be considered: thickness and thermal conductivity of the material. The thermal conductivity is a material characteristic that illustrates its ability to conduct heat. It is a constant value that is not be affected by the thickness of the material (Bienvenido-Huertas et al., 2019a). U-value can be considered as the inverse of the thermal resistance (Gaspar et al., 2016). The thermal resistance of a material is a value that the thickness divided by thermal conductivity of this material (Bienvenido-Huertas et al., 2019b). If thermal conductivity is low and/or thickness of material is large, high thermal resistance of material can be achieved and then low U-values can also be achieved. Table 2 shows the U-values of some common walls and glazing materials.

Table 2
U-values of some common walls and glazing materials.

Ref.	Material	U-value
Wong and Chan (2012)	Softwood	0.13
	Hardwood	0.18
	Brick	0.77
	Normal concrete (2400 kgm^{-3})	1.93
Cuce and Riffat (2015a)	Vacuum glazing	0.7
Cuce and Riffat (2015b)	Aerogel glazing	0.67
Cuce and Riffat (2015c)	Air filled-double-glazed window with low-e	2.1
Citherlet et al. (2000)	TIM (Transparent insulation material) glazing	1.17

Table 3
PDMG Facade area of walls and roof area.

Walls	W (m)	L (m)	Area (m^2)
N	0.86	1.18	1.0148
S	0.86	1.18	1.0148
W	1.13	1.01	1.1413
E	1.13	1.18	1.3334
Roof	0.7	1.00	0.7

Table 5
Related readings about relative humidity and temperature difference.

Reading	RH (%)	Δ**T** (°C)
Average	76.94	−1.21
Max	99.9	31.5
Min	53.8	−35

2.2. Shading coefficient (SC)

In a shading system, the shading coefficient is the product of two subsystems from the shading coefficients. The simple equation is shown in (15) (Ezzaeri et al., 2018),

$$SC = SC_1 \times SC_2 \quad (15)$$

Where
SC is effective shading coefficient of fenestration system,
SC_1 is shading coefficient of subsystem 1 i.e. glass,
SC_2 is shading coefficient of subsystem 2 i.e. external shading devices.

The shading coefficient of the glass measures the total solar gain through the glass. It relies on the glass color and the degree of reflectivity. SC ranges from 0 to 1, which is a major contributor to the OTTV (Northern and Seminar, 2016). A low SC value indicates that less solar heat gain pass through the glass (Wong and Chan, 2012). The shading coefficient of the external shading devices measures the solar control of a shading, which is used for limiting the radiant and re-radiant solar gain (Natephra et al., 2018).

Shading coefficient can be defined based on shading devices allocation, which is normally applied on horizontal or/and vertical. These shading devices are able to help reducing solar heat gain through windows.

However, in this study it is obvious from Fig. 6(a) that there is no external shading device used for the PDMG roof. The solar radiation is then directly transmitted through the semi-transparent roof without any shading. Therefore, the shading coefficient of external shading device can be reasonably assumed as 1 with the assumption that glass cover has no shading coefficient. Furthermore, based on the OTTV calculation, SC is only considered for window glass. So it is unnecessary for walls of PDMG to use shading coefficient in this research because of no window glasses in the structure of walls of PDMG.

3. Methodology

3.1. The façade area and construction profile of PDMG

The section shows detailed methodology in terms of OTTV calculation details needed for the PDMG assessment. In order to evaluate OTTV on the PDMG, MS1525:2014 per Eq. (2) for the wall and Eq. (3) for the roof are selected as main equations and each parameter required are investigated. The Portable DSSC Mini Greenhouse structure is defined as orientation North, South, East and West. The sizes of the façade area (one exterior side of a building) for the walls and the roof area are defined in Table 3. It is noted that there were four Red Colored DSSC modules (DSS SERIO 3550W19 Solaronix, Switzerland) fixed as the roof. The size of each DSSC module is 0.35 m × 0.5 m. Fig. 6 shows the detailed construction of PDMG and the practical arrangement of PDMG system.

Here are key elements of the PDMG prototype in Fig. 6(a):

(i) Shading greenhouse is used to reduce intensity of solar radiation (especially in hot and tropical regions) in order to achieve appropriate environment for plants and crops.
(ii) The red color of DSSC (determined by the dye) can act as photoselective shading which can modify the solar spectrum. Thus, the photosynthesis & photomorphogenesis increases plant growth capabilities.
(iii) Provide castor wheel at the bottom of the PDMG in order to get optimum sunlight: Portability feature.
(iv) Eliminates the negative effects of the seasonal elevation of sun & reduction of the PAR that is required for photosynthesis: In order to get optimum sunlight.
(v) Adjustable racking system provides various types of crops and sizes of plant to be fixing into the mini greenhouse.
(vi) wall of PDMG can be changed accordingly (present: mesh wall's greenhouse will be substituted or changed in the

Table 4
Positive effect of red light on plants.

Ref.	Plant	Radiation source	Effect on plant
Lu et al. (2012)	Tomato (*Lycopersicum esculentum* L. cv. MomotaroNatsumi)	Red (660 nm) LEDs	Tomato yield increased
Mizuno et al. (2011)	Cabbage (*Brassicaolearacea var. capitata* L.)	Red (660 nm) LEDs	Anthocyanin content increased
Dou et al. (2017)	Grape (*Vitis vinifera cv. 'Jingxiu'*)	Supplementary red light in a greenhouse	The leaf area of grape increased

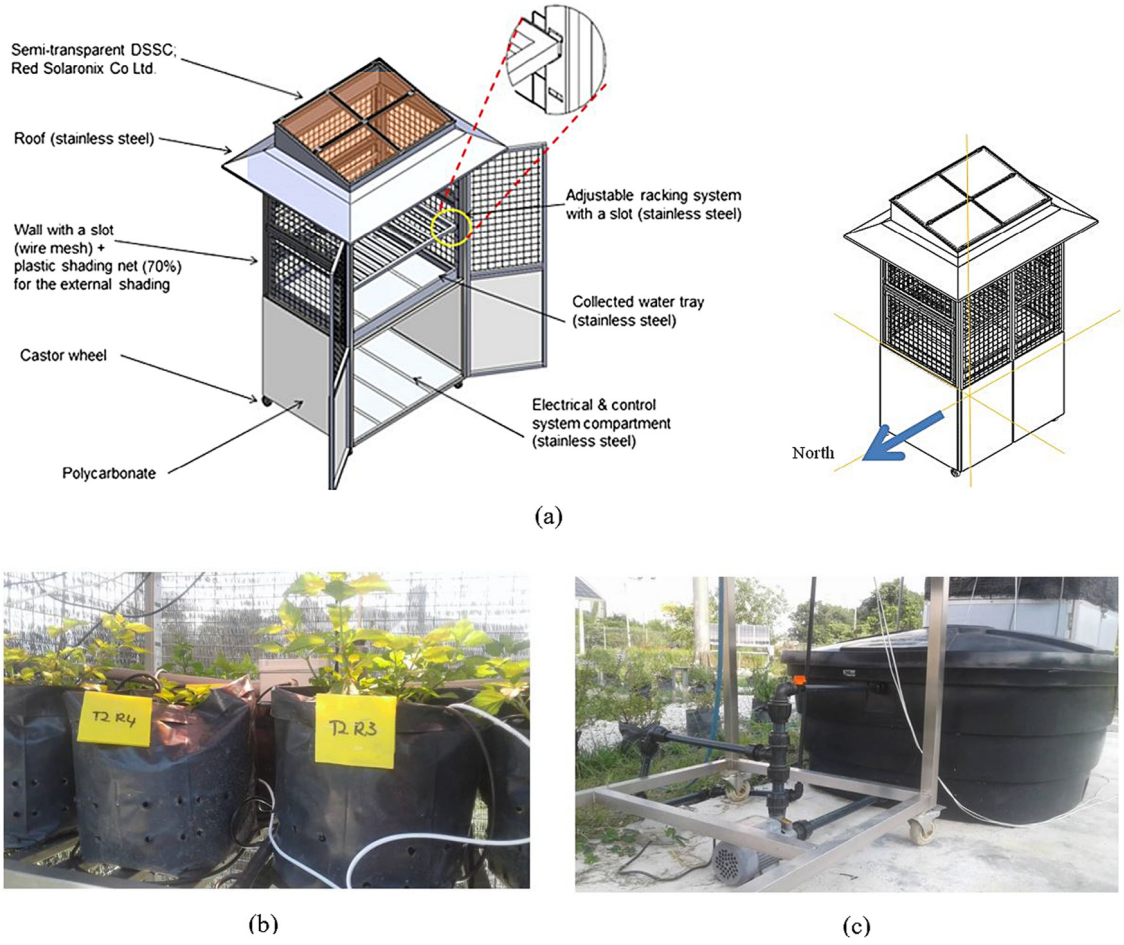

Fig. 6. (a) The detailed construction drawings of PDMG prototype and (b) fertigation and (c) irrigation close loop PDMG system.

future with other materials e.g. Closed polycarbonate/glass/net wall of greenhouse).

Furthermore, Fig. 6(b) and (c) present the practical arrangements of fertigation and irrigation close loop PDMG system respectively. The plant presented in Fig. 6(b) is *orthosiphon stamineus*, which is commonly known as "Misai Kucing" (Malaysian). It has extensively medical uses and mostly e.g. its leaves are applied to treat diabetes, lithiasis, rheumatoid diseases, edema, tonsillitis, influenza, eruptive fever etc. (Ameer et al., 2012). The botanical drug is defined as a botanical product that is marketed as treating or curing a disease (Wikipedia, 2019) e.g. infectious disease. As mentioned in Section 1.2, the ingredients of botanical drugs come from plant parts etc. and herbal products can be extracted as the botanical drugs. The Portable DSSC Mini Greenhouse is relatively high in terms of the materials and structure. Thus, it should produce or specify high value herbal crops (HVHC). In Fig. 7, Misai Kucing (red circle) has been selected as HVHC for EPP1 program in Malaysia (Othman et al., 2016).

In this research, due to red colored DSSC as roof in the mini greenhouse, then red light plays an important role in the plants cultivated in the DSSC greenhouse system. The red light, which is radiation with wavelengths between 620 nm and 750 nm, has a pronounced and positive effect on the plant growth e.g. increasing photosynthesis rate and plant size (Nielsen, 2018). It is known that red light wavelengths ideally fit the absorption peak of chlorophylls and phytochromes so that red light on plant growth can reach the high efficiency (Dou et al., 2017). Several reports (Table 4) have shown that red light is good for plants. However, this research focused on the heat dissipation through DSSC roof based on OTTV method. Regarding the effect of red light towards plant growth in this mini DSSC greenhouse, next research will be targeted.

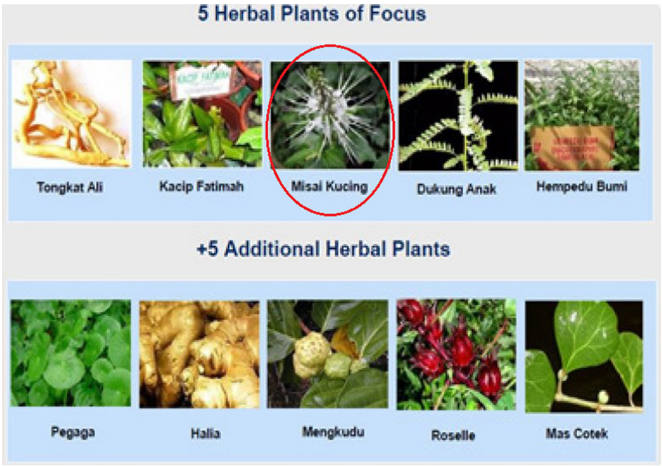

Fig. 7. The selected herbal plants for EPP1 program.
Source: From http://www.moa.gov.my.

3.2. System block diagram and electrical output

Fig. 8 illustrates the complete system block diagram. Fig. 8(a) shows DSSC greenhouse data logging and irrigation system block

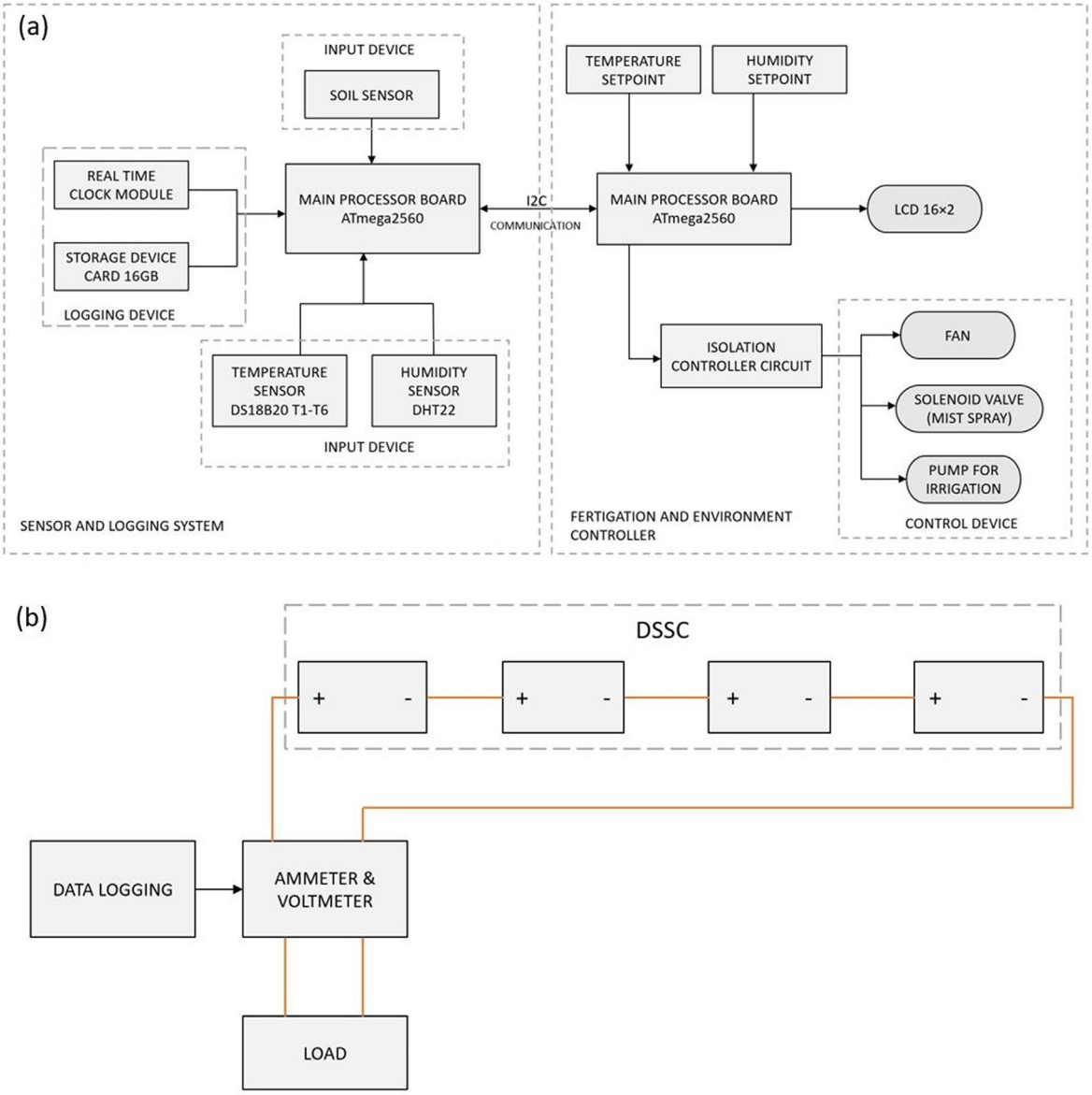

Fig. 8. The whole system block diagram.

diagram. Two systems (sensor and logging system), (fertigation and environment controller system) operated at the same time-stamp based on the I2C communication protocol to send and receive data (Data Management System). Fig. 8(b) shows DSSC connection for data acquisition schematic. Four Red colored DSSC modules were connected in series. Solar Module Analyzer (PROVA 210) data logging device was used for performing DSSC electrical output. The information of related devices was attached in Appendix. The DSSC electrical characteristic for Module SERIO3550W19 in Fig. 9.

The red curve in Fig. 9 shows the DSSC electrical (I–V) characteristic for Module SERIO3550W19. With the solar radiation (666 Wm^{-2}), the DSSC reaches the peak electric power at 1.7 W. Besides, Fig. 10 (Roslan et al., 2019) presents the electrical characteristics of DSSC module based on Malaysia weather.

Fig. 10(a) shows power energy generated from semi-transparent DSSC mini greenhouse for 5 days. With the increasing of solar radiation, generated power also gradually increased, and vice versa. The peak value of generated electric power ranged from 1.783 W to 2.081 W. The average electric power generated between 0.532 W and 0.828 W. Fig. 10(b) shows efficiency and Fill Factor (FF) of DSSC module. The efficiency of a PV module is defined as the ratio between energy output from the module and input energy from the sunlight. It can be seen that the maximum value of efficiency reached at 2.907% and the average value of efficiency was ranged from 0.848% to 1.503% during the observation. FF is the ratio of maximum obtainable power under normal operating condition to the product of open-circuit voltage (V_{OC}) and short-circuit current (I_{SC}). From Fig. 10(b), the maximum value of FF was ranged from 1.109 to 1.148, and also average value of FF ranged between 0.381 and 0.388 during the observation (Roslan et al., 2019).

3.3. Equation simplification for the OTTV roof

For the roof, there is no opaque material used for covering the roof. It can be seen from Fig. 6(a) DSSC greenhouse profile that the covering material of roof is only semi-transparent DSSC. It can be considered as the skylight area, so the OTTV calculation only needs to consider two components: heat conduction transmitted through the skylight area and solar radiation transmitted through

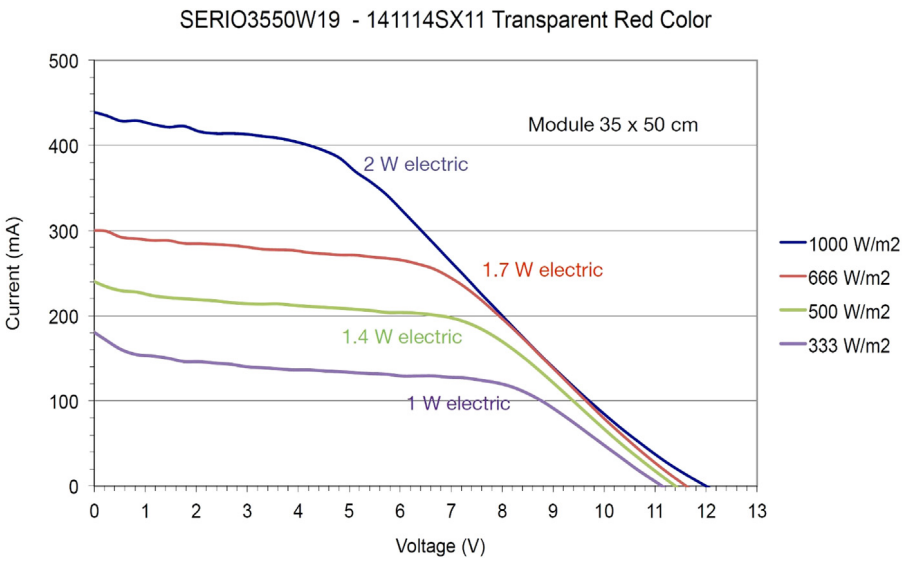

Fig. 9. The DSSC electrical characteristic for Module SERIO3550W19.. (For interpretation of the references to color in this figure legend, the reader is referred to the web version of this article.)
Source: From Solaronix, Switzerland.

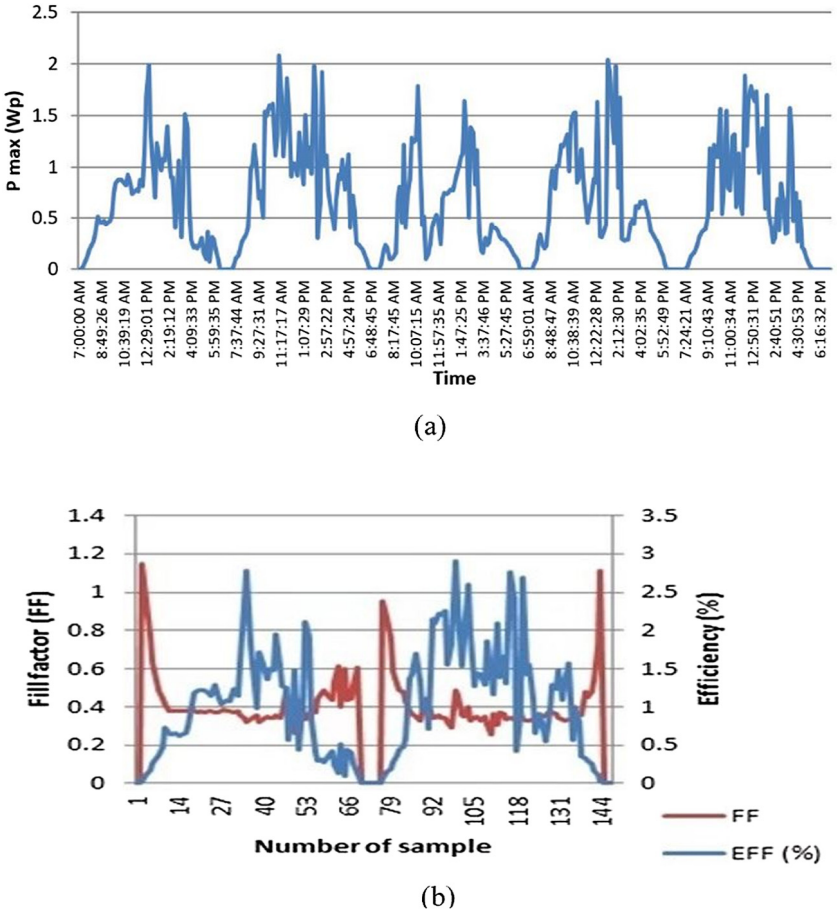

Fig. 10. The electrical output (a) electric power energy generated from DSSC module in mini greenhouse for five days and (b) efficiency and fill factor (FF) of DSSC module (Roslan et al., 2019).

the skylight area. Using Eq. (3), the calculation formula for the OTTV roof can be simplified as (16).

$$OTTV_r = \frac{(A_s \times U_s \times \Delta T) + (A_s \times SC \times SF)}{A_s} \tag{16}$$

Where
SF is defined by Energy efficiency and use of renewable energy for non-residential buildings (2014)

$$SF = 323 \times OF \tag{17}$$

Table 6
The OTTV value for walls of PDMG.

Heat conduction through HDPE							
Elevation	Façade Area	Constant	α_1	$(1-WWR)_1$	U_1	$OTTV_1$	$A \times OTTV_1$
North	1.0148	15	0.9	0.7	470	4441.5	4507.23
South	1.0148	15	0.9	0.7	470	4441.5	4507.23
East	1.3334	15	0.9	0.7	470	4441.5	5922.30
West	1.1413	15	0.9	0.7	470	4441.5	5069.08
HDPE $OTTV_T$	4.5043	$15 \times \alpha_1 \times (1-WWR)_1 \times U_1$					20005.84
Heat conduction through stainless steel							
Elevation	Façade area	Constant	α_2	$(1-WWR)_2$	U_2	$OTTV_2$	$A \times OTTV_2$
North	1.0148	15	0.5	0.12	1.31	1.18	1.20
South	1.0148	15	0.5	0.12	1.31	1.18	1.20
East	1.3334	15	0.5	0.12	1.31	1.18	1.57
West	1.1413	15	0.5	0.12	1.31	1.18	1.35
SS $OTTV_T$	4.5043	$15 \times \alpha_2 \times (1-WWR)_2 \times U_2$					5.32
Wall $OTTV_T$	4.5043					4442.68	20011.16

Based on MS1525:2014, the DSSC roof facing orientation is south with 15° slope angle, so *OF* for the roof is 1.

3.4. Assumption of U-values

In this study, wall of PDMG has two parts: external plastic shading and the stainless-steel frame structure of PDMG. There is no window glass used in the wall of PDMG, so OTTV calculation for wall of PDMG only considers heat conduction through opaque wall. The material of external plastic shading is black glossy high-density polyethylene (HDPE), in the form of 70 percent shading net. The thickness of this material used in this study is 1 mm. Definition of thermal conductivity k under CAS: 25213-02-9, giving value of 0.47 $Wm^{-1}K^{-1}$. Using Eqs. (18) and (19), U-value of the HDPE is 470 $Wm^{-2}K^{-1}$. Besides, the total thickness of stainless-steel (Type 304) is 24 mm. In order to calculate U-value of stainless-steel, stainless-steel should be divided into three layers because stainless-steel is hollow. The first and third layer are both stainless-steel, the thickness and thermal conductivity are both 2 mm and 14.4 $Wm^{-1}K^{-1}$ (Calculator et al., 2012) respectively. The second layer is air, the thickness and thermal conductivity are 20 mm and 0.0262 $Wm^{-1}K^{-1}$ (Calculator et al., 2012). Based on Eqs. (18) and (19), U-value of 24 mm stainless-steel is around 1.31 $Wm^{-2}K^{-1}$.

Moreover, the main element of the DSSC roof is polycarbonate, so the thermal conductivity of the DSSC can be approximately assumed as the thermal conductivity of the polycarbonate, which is 0.19 $Wm^{-1}K^{-1}$ (Calculator et al., 2012). The thickness of this DSSC is 3.9 mm and then U-value for the DSSC roof will be around 48.72$Wm^{-2}K^{-1}$.

U-values is defined by

$$U = \frac{1}{R_{total}} \tag{18}$$

Where, R is thermal resistance defined by

$$R = \frac{material\ thickness, l\ (\mathrm{m})}{thermal\ conductivity, k\ (\mathrm{Wm^{-1}K^{-1}})} \tag{19}$$

3.5. Locations of humidity and temperature sensors

Fig. 11 displays the location of the humidity sensor and the locations of temperature sensors from side view and top view respectively of PDMG in order to view properly. The pink round dot in the left picture of Fig. 11 stands for location of humidity sensor from side view, which lies at 0.6 m distance from DSSC roof of PDMG. In the right picture of Fig. 11, the red-round-dot and the blue-star both represent temperature sensors. From top view, they are located at the upper surface (red-round-dot) of DSSC roof and at the bottom surface (blue-star) of DSSC roof respectively.

Table 7
The OTTV value for roof of PDMG.

Heat conduction through skylight					
A_s	U_s	ΔT	SC	SF	OTTV
0.7	48.72	1.21	–	–	41.38
Solar radiation through skylight					
0.7	–	–	1	323	226.1
Total OTTV of roof					
0.7	$\frac{A_s \times U_s \times \Delta T + A_s \times SC \times SF}{A_s}$				382.12

4. Results and discussion

4.1. Humidity and temperature difference

From Fig. 11, the humidity (%) was recorded by humidity sensor at 0.6 m distance from DSSC panel inside the PDMG in this research. The temperature difference ΔT is defined as the difference value between upper surface temperature of DSSC and bottom surface temperature of DSSC, their values were recorded by the temperature sensors respectively. The tested time was from 7am to 7pm for randomly 5 days during April 2019. Fig. 12 shows humidity for 5 days inside the PDMG and temperature difference through DSSC roof material for 5 days.

Besides, the maximum and minimum values of temperature difference are 31.5 °C and −35 °C respectively among five days. The average temperature difference value for five days shows about −1.21 °C, and it means that the temperature at the bottom surface of DSSC is higher than that at the upper surface of DSSC on average level between 7am and 7pm. It can be seen from Fig. 12 that relative humidity reaches the highest level when the temperature difference between the upper surface of DSSC and the bottom surface of DSSC lies at the minimum level and vice versa. It is noted that only in Fig. 12 the absolute values of temperature difference ΔT were displayed in order to show pattern clearly e.g. the minimum ΔT (−35 °C) was taken positive value 35 °C in the graph. Table 5 shows the related readings about relative humidity and temperature difference. Then, the absolute value of average ΔT would be applied to OTTV roof calculation.

4.2. Overall thermal transfer value of PDMG

Table 6 shows the OTTV results for walls of PDMG. As mentioned in Section 3.4, OTTV calculation for walls only considers opaque walls due to absence of windows. Hence, OTTV calculation is composed of heat conduction through HDPE and heat

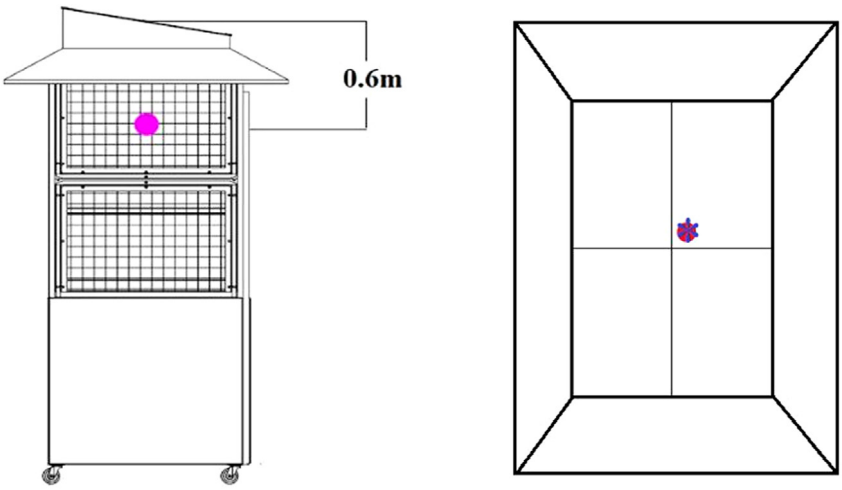

Fig. 11. The location of Humidity sensor from side view (left picture) and the locations of temperature sensors from top view of PDMG (right picture).

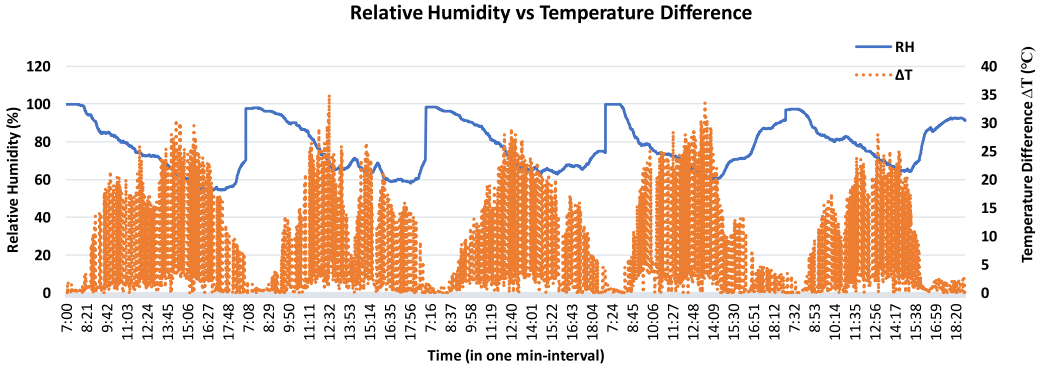

Fig. 12. Relative Humidity & ΔT for 5 days in one min-interval during April 2019.

conduction through stainless steel. The definition of *WWR* is ratio between gross area of windows and gross areas of all walls, then (1 − *WWR*) is ratio between gross area of opaque walls and gross areas of all walls. Based on this definition, in this research from Fig. 6(a) describes that 70% of walls is external shading and remaining 30% of walls allows air flow. Herein (1 − *WWR*) for HDPE can be considered as 0.7. The gross area of stainless steel is around 0.53 m^2, so (1 − *WWR*) for stainless steel can be considered as 0.12. It is clear that the final OTTV for walls of PDMG is calculated as 4442.68 Wm^{-2}. Most of the heat gain for walls of PDMG comes from heat conduction through HDPE. This is because U-value contributes to high heat conduction through HDPE. Solar absorptivity e.g. black color also has a significant effect on heat conduction through HDPE.

Table 7 shows the OTTV result for two components of roof: total heat conduction through skylight is about 41.38 Wm^{-2} and total solar radiation through skylight is 226.1 Wm^{-2}. The final OTTV value for roof of PDMG is calculated as 382.12 Wm^{-2}.

Therefore, overall OTTV for PDMG is about 4824.8 Wm^{-2}.

5. Conclusion and recommendation

This paper has investigated the calculation of the Overall Thermal Transfer Value (OTTV) for Portable DSSC Mini Greenhouse (PDMG) at the UPM in Malaysia. Even though the OTTV was mainly developed for the air-conditioned building, it can also work as a useful indicator for non-air-conditioned buildings to estimate the amount of heat transfer gain into the building envelope especially for greenhouse. This is because heat stress to plants in the greenhouse can be reasonably reduced based on OTTV evaluation from outer layer construction of greenhouse. OTTV approach is especially important in tropical countries or sub-tropical regions e.g. Malaysia, Singapore, Thailand and Hong Kong of China. Different countries or regions have different OTTV calculations, which includes different parameters in the OTTV equations based on the local context. The idea is that OTTV method is firstly applied to greenhouse because botanical drugs play a critical role in medical and economical aspects. The growth environment of botanical drugs can always be affected by heat stress from sunlight, so heat stress is a practical issue in tropical countries. Most of plants in the greenhouse grow best when the light wavelength band lies between 400 and 700 nm (PAR) that is best solar spectrum band for photosynthesis process. Then OTTV approach is a reliable tool to estimate the total heat gain transmit through greenhouse envelope in order to provide thermal analysis on the construction of greenhouse. Heat stress then can be reasonably avoided based on OTTV evaluation. In this paper, the calculation of OTTV for PDMG consists of two parts: one calculation is for walls of PDMG and the other calculation is for DSSC roof of PDMG. Based on the OTTV equations from Malaysia Standard MS1525:2014, OTTV result for the walls were found to be 4442.68 Wm^{-2}. OTTV equation for the roof was simplified due to semi-transparent DSSC as the roof, then 382.12 Wm^{-2} was calculated for OTTV roof. The total OTTV of PDMG is around 4824.8 Wm^{-2}. Hence, this PDMG is a practical design that is used for thermal analysis by using OTTV approach.

In the future, different materials should be used for outer layer of PDMG envelope through OTTV methods to find out the better

growth environment for botanical drugs. Besides, OTTV method can also be applied for further thermal analysis research in other PV greenhouses.

Declaration of competing interest

The authors declare that they have no known competing financial interests or personal relationships that could have appeared to influence the work reported in this paper.

Acknowledgments

The authors delegate our thanks to the Research Management Centre (RMC), Universiti Putra Malaysia for the approval of research funding under the IPB Putra Grants Scheme (Vote no: 9515303) and IPS Putra Grants Scheme (Vote no: 9606500).

Appendix

Controller device:
1 x MCU 8-bit *Data bus, 16 MHz Clock, 256* kB *Program memory, 8* kB *SRAM*
2 x MCU 8-bit *Data bus, 16 MHz Clock, 32* kB *Program memory, 2* kB *SRAM, 1* kB

EEPROM:
Dallas Semiconductor 12-bit *DS18B20 temperature sensor,* −55 °C to +125 °C
Bosch BME280 humidity and pressure sensor, −40 to +85 °C, *RH* 0%–100%, *Pressure 300–1100* hPa
Soil Resistance based Soil Sensor
16 × 2 Hitachi compatible liquid crystal display (LCD)

Memory:
SanDisk Ultra microSDHC Card UHS-I Class 10 (80 MB/s) *16* GB, *IEC 529 IPX7, −25* °C *to 85* °C, *able to withstand 500* Gs *shock, X-ray proof and magnetic proof*

System:
1-min *interval real time logging with capability to be expanded with a Local Area Network (LAN)*
1-unit controllable temperature set point
1-unit controllable humidity set point
1-unit controllable soil moisture set point (internal)

Device controlled:
12 VDC 80 W *exhaust fan*
Mist spray system
1/2 HP water pump

References

Abdelrazik, A.S., Al-Sulaiman, F.A., Saidur, R., Ben-Mansour, R., 2018. A review on recent development for the design and packaging of hybrid photovoltaic/thermal (PV/T) solar systems. Renew. Sustain. Energy Rev. 95, 110–129. http://dx.doi.org/10.1016/j.rser.2018.07.013.

Adedokun, O., Titilope, K., Awodugba, A.O., 2016. Review on natural dye-sensitized solar cells (DSSCs). Int. J. Eng. Technol. IJET 2, 34. http://dx.doi.org/10.19072/ijet.96456.

Ahn, K., 2017. The worldwide trend of using botanical drugs and strategies for developing global drugs, 50. pp. 111–116.

Ameer, O.Z., Salman, I.M., Asmawi, M.Z., Ibraheem, Z.O., Yam, M.F., 2012. Orthosiphon stamineus: Traditional uses, phytochemistry, pharmacology, and toxicology. J. Med. Food 15, 678–690. http://dx.doi.org/10.1089/jmf.2011.1973.

Anon, 1992. A sean- usa id buildings energy conservation project final report volume I: Energy standards.

Anon, 1995. Code of Practice for Overall Thermal Transfer Value in Building, . Building Authority Hong Kong.

Anon, 2017a. Asia pacific botanical & plant derivative drug market forecast 2018–2026. Inkwood Res. https://www.inkwoodresearch.com/reports/asia-pacific-botanical-and-plant-derivative-drug-market/. (Accessed 28 September 2019).

Anon, 2017b. Europe botanical & plant derivative drug market forecast 2018–2026. Inkwood Res. https://www.inkwoodresearch.com/reports/europe-botanical-and-plant-derivative-drug-market/. (Accessed 28 September 2019).

Anon, 2017c. North america botanical & plant derivative drug market forecast 2018–2026. Inkwood Res. https://www.inkwoodresearch.com/reports/north-america-botanical-plant-derivative-drug-market/. (Accessed 28 September 2019.

Bienvenido-Huertas, D., Moyano, J., Marín, D., Fresco-Contreras, R., 2019a. Review of in situ methods for assessing the thermal transmittance of walls. Renew. Sustain. Energy Rev. 102, 356–371. http://dx.doi.org/10.1016/j.rser.2018.12.016.

Bienvenido-Huertas, D., Moyano, J., Rodríguez-Jiménez, C.E., Marín, D., 2019b. Applying an artificial neural network to assess thermal transmittance in walls by means of the thermometric method. Appl. Energy 233–234, 1–14. http://dx.doi.org/10.1016/j.apenergy.2018.10.052.

Botanical and Plant Derived Drugs Market, 2019. Latest innovations, Drivers and industry key events 2015–2023. https://onyourdesks.com/2019/09/21/botanical-and-plant-derived-drugs-market-latest-innovations-drivers-and-industry-key-events-2015-2023/. (Accessed 26 September 2019).

Calculator, G., Removal, W., Cylinder, G., 2012. Thermal conductivity of some common materials and gases thermal conductivity of some common materials and gases page 2 of 5. pp. 2–6.

Castellano, S., Santamaria, P., Serio, F., 2016. Solar radiation distribution inside a monospan greenhouse with the roof entirely covered by photovoltaic panels. J. Agric. Eng. 47, 1–6. http://dx.doi.org/10.4081/jae.2016.485.

Chan, A.L.S., 2018. Evaluating the impact of photovoltaic systems on the thermal performance of buildings and its implication to building energy code. A case study in subtropical Hong Kong. Energy Policy 119, 674–688. http://dx.doi.org/10.1016/j.enpol.2018.04.041.

Chan, L.S., 2019. Investigating the environmental effectiveness of Overall Thermal Transfer Value code and its implication to energy regulation development. Energy Policy 130, 172–180. http://dx.doi.org/10.1016/j.enpol.2019.04.004.

Chan, A.L.S., Chow, T.T., 2013. Evaluation of overall thermal transfer value (OTTV) for commercial buildings constructed with green roof. Appl. Energy 107, 10–24. http://dx.doi.org/10.1016/j.apenergy.2013.02.010.

Chan, A.L.S., Chow, T.T., 2014. CaLculation of overall thermal transfer value (OTTV) for commercial buildings constructed with naturally ventilated double skin façade in subtropical Hong Kong. Energy Build. 69, 14–21. http://dx.doi.org/10.1016/j.enbuild.2013.09.049.

Chen, S., Huang, Y., Weng, J., Fan, X., Mo, L., Pan, B., Dai, S., 2013. Numerical model analysis of thermal performance for a dye-sensitized solar cell module. J. Phys. D: Appl. Phys. 46 (48), 485106.

Chirarattananon, S., Chaiwiwatworakul, P., Hien, V.D., Rakkwamsuk, P., Kubaha, K., 2010. Assessment of energy savings from the revised building energy code of Thailand. Energy 35, 1741–1753. http://dx.doi.org/10.1016/j.energy.2009.12.027.

Chua, K.J., Chou, S.K., 2010. An ETTV-based approach to improving the energy performance of commercial buildings. Energy Build. 42, 491–499. http://dx.doi.org/10.1016/j.enbuild.2009.10.018.

Chua, K.J., Chou, S.K., 2011. A performance-based method for energy efficiency improvement of buildings. Energy Convers. Manage. 52, 1829–1839. http://dx.doi.org/10.1016/j.enconman.2010.12.007.

Citherlet, S., Di Guglielmo, F., Gay, J.B., 2000. Window and advanced glazing systems life cycle assessment. Energy Build. 32, 225–234. http://dx.doi.org/10.1016/S0378-7788(98)00073-5.

Consumption, A.E., 2009. Green building index – Ms1525 1 factors affecting energy use in.

Cossu, M., Cossu, A., Deligios, P.A., Ledda, L., Li, Z., Fatnassi, H., Poncet, C., Yano, A., 2018. Assessment and comparison of the solar radiation distribution inside the main commercial photovoltaic greenhouse types in Europe. Renew. Sustain. Energy Rev. 94, 822–834. http://dx.doi.org/10.1016/j.rser.2018.06.001.

Cuce, E., 2018. Energy & buildings accurate and reliable u -value assessment of argon-filled double glazed windows, : A numerical and experimental investigation. Energy Build. 171, 100–106. http://dx.doi.org/10.1016/j.enbuild.2018.04.036.

Cuce, E., Riffat, S.B., 2015a. A state-of-the-art review on innovative glazing technologies. Renew. Sustain. Energy Rev. 41, 695–714. http://dx.doi.org/10.1016/j.rser.2014.08.084.

Cuce, E., Riffat, S.B., 2015b. Aerogel-assisted support pillars for thermal performance enhancement of vacuum glazing: A CFD research for a commercial product. Arab. J. Sci. Eng. 40, 2233–2238. http://dx.doi.org/10.1007/s13369-015-1727-5.

Cuce, E., Riffat, S.B., 2015c. Vacuum tube window technology for highly insulating building fabric: An experimental and numerical investigation. Vacuum 111, 83–91. http://dx.doi.org/10.1016/j.vacuum.2014.10.002.

Devgan, S., Jain, A.K., Bhattacharjee, B., 2010. Predetermined overall thermal transfer value coefficients for composite, Hot-Dry and Warm-Humid climates. Energy Build. 42, 1841–1861. http://dx.doi.org/10.1016/j.enbuild.2010.05.021.

Djamila, H., Rajin, M., Rizalman, A.N., 2018. Energy efficiency through building envelope in Malaysia and Singapore. J. Adv. Res. Fluid Mech. Therm. Sci. 46, 96–105, https://www.scopus.com/inward/record.uri?eid=2-s20-85048659998&partnerID=40&md5=0959aca7165ab2de9f176f2df35c6db6.

Dou, H., Niu, G., Gu, M., Masabni, J.G., 2017. Effects of light quality on growth and phytonutrient accumulation of herbs under controlled environments. Horticulturae 3, 1–11. http://dx.doi.org/10.3390/horticulturae3020036.

Du, Y., Tao, W., Liu, Y., Jiang, J., Huang, H., 2017. Heat transfer modeling and temperature experiments of crystalline silicon photovoltaic modules. Sol. Energy 146, 257–263. http://dx.doi.org/10.1016/j.solener.2017.02.049.

Energy efficiency and use of renewable energy for non-residential buildings, 2014. Code of practice (Second Revision), Malaysian stand. MS15252014.

Ezzaeri, K., Fatnassi, H., Bouharroud, R., Gourdo, L., Bazgaou, A., Wifaya, A., Demrati, H., Bekkaoui, A., Aharoune, A., Poncet, C., Bouirden, L., 2018. The effect of photovoltaic panels on the microclimate and on the tomato production under photovoltaic canarian greenhouses. Sol. Energy 173, 1126–1134. http://dx.doi.org/10.1016/j.solener.2018.08.043.

Fernandes, M.S., Rodrigues, E., Gaspar, A.R., Costa, J.J., Gomes, Á, 2019. The impact of thermal transmittance variation on building design in the Mediterranean region. Appl. Energy 239, 581–597. http://dx.doi.org/10.1016/j.apenergy.2019.01.239.

Gao, Y., Dong, J., Isabella, O., Santbergen, R., Tan, H., Zeman, M., Zhang, G., 2019. Modeling and analyses of energy performances of photovoltaic greenhouses with sun-tracking functionality ⋆. Appl. Energy 233–234, 424–442. http://dx.doi.org/10.1016/j.apenergy.2018.10.019.

Gaspar, K., Casals, M., Gangolells, M., 2016. A comparison of standardized calculation methods for in situ measurements of façades U-value. Energy Build. 130, 592–599. http://dx.doi.org/10.1016/j.enbuild.2016.08.072.

Ghani, S., Bakochristou, F., Mohamed, E., Ahmed, A., Mahmoud, S., Gamaledin, A., Rashwan, M.M., 2019. Engineering in agriculture, Environment and food design challenges of agricultural greenhouses in hot and arid environments – A review. Eng. Agric. Environ. Food 12, 48–70. http://dx.doi.org/10.1016/j.eaef.2018.09.004.

Goldman, P., 2001. Herbal medicines today and the roots of modern pharmacology, 135. pp. 594–600.

Hammam, M., El-mansy, M.K., El-bashir, S.M., El-shaarawy, M.G., 2007. Performance evaluation of thin-film solar concentrators for greenhouse applications, 209. pp. 244–250. http://dx.doi.org/10.1016/j.desal.200704034.

Harun, M.F., Samah, A.A., Majid, H.A., Yusoff, Y., Lim, Y.W., 2017. Optimization of green building design to achieve green building index (GBI) using genetic algorithm (GA). In: 6th ICT Int. Student Proj. Conf. Elev. Community Through ICT, ICT-ISPC 2017. pp. 1–4. http://dx.doi.org/10.1109/ICT-ISPC.2017.8075310.

Hassanien, R.H.E., Li, M., Dong Lin, W., 2016. Advanced applications of solar energy in agricultural greenhouses. Renew. Sustain. Energy Rev. 54, 989–1001. http://dx.doi.org/10.1016/j.rser.2015.10.095.

Hussein, A.M., Iefanova, A.V., Koodali, R.T., Logue, B.A., Shende, R.V., 2018. Interconnected ZrO_2 doped ZnO/TiO_2 network photoanode for dye-sensitized solar cells. Energy Rep. 4, 56–64. http://dx.doi.org/10.1016/j.egyr.2018.01.007.

Hwang, R.L., Shih, W.M., Lin, T.P., Huang, K.T., 2018. Simplification and adjustment of the energy consumption indices of office building envelopes in response to climate change. Appl. Energy 230, 460–470. http://dx.doi.org/10.1016/j.apenergy.2018.08.090.

Iwata, S., ichiro Shibakawa, S., Imawaka, N., Yoshino, K., 2018. Stability of the current characteristics of dye-sensitized solar cells in the second quadrant of the current–voltage characteristics. Energy Rep. 4, 8–12. http://dx.doi.org/10.1016/j.egyr.2017.10.004.

Jia, J., Lee, W.L., 2018. The rising energy efficiency of office buildings in Hong Kong. Energy Build. 166, 296–304. http://dx.doi.org/10.1016/j.enbuild.2018.01.062.

Kadowaki, M., Yano, A., Ishizu, F., Tanaka, T., Noda, S., 2012. Effects of greenhouse photovoltaic array shading on Welsh onion growth. Biosyst. Eng. 111, 290–297. http://dx.doi.org/10.1016/j.biosystemseng.2011.12.006.

Kakooza-mwesige, A., 2015. Epilepsy & behavior the importance of botanical treatments in traditional societies and challenges in developing countries. Epilepsy Behav. 52, 297–307. http://dx.doi.org/10.1016/j.yebeh.2015.06.017.

Kane, S.N., Mishra, A., Dutta, A.K., 2016. Efficiency enhancement of dye-sensitized solar cells (DSSC) by addition of synthetic dye into natural dye (anthocyanin). J. Phys. Conf. Ser. 755 (2016), 8–14. http://dx.doi.org/10.1088/1742-6596/755/1/011001.

Khanna, S., Sundaram, S., Reddy, K.S., Mallick, T.K., 2017. Performance analysis of perovskite and dye-sensitized solar cells under varying operating conditions and comparison with monocrystalline silicon cell. Appl. Therm. Eng. 127, 559–565. http://dx.doi.org/10.1016/j.applthermaleng.2017.08.030.

Kim, J.J., Kang, M., Kwak, O.K., Yoon, Y.J., Min, K.S., Chu, M.J., 2014. Fabrication and characterization of dye-sensitized solar cells for greenhouse application. Int. J. Photoenergy 2014, http://dx.doi.org/10.1155/2014/376315.

Kim, N., Kim, D., Kang, H., Park, Y.G., 2016. Improved heat dissipation in a crystalline silicon PV module for better performance by using a highly thermal conducting backsheet. Energy 113, 515–520. http://dx.doi.org/10.1016/j.energy.2016.07.046.

Kumar, K.S., Tiwari, K.N., Jha, M.K., 2009. Design and technology for greenhouse cooling in tropical and subtropical regions: A review. Energy Build. 41, 1269–1275. http://dx.doi.org/10.1016/j.enbuild.2009.08.003.

Lamnatou, C., Chemisana, D., 2013. Solar radiation manipulations and their role in greenhouse claddings, : Fresnel lenses, NIR- and UV-blocking materials. Renew. Sustain. Energy Rev. 18, 271–287. http://dx.doi.org/10.1016/j.rser.2012.09.041.

Liu, Y., Wang, M.W., 2008. Botanical drugs: Challenges and opportunities. In: Contribution to Linnaeus Memorial Symposium 2007. In: Life Sci., 82, pp. 445–449. http://dx.doi.org/10.1016/j.lfs.2007.11.007.

Lu, N., Maruo, T., Johkan, M., Hohjo, M., Tsukagoshi, S., Ito, Y., Ichimura, T., Shinohara, Y., 2012. Effects of supplemental lighting with light emitting diodes (LEDs) on tomato yield and quality of single truss tomato plants grown at high planting density. Environ. Control Biol. 50, 63–74. http://dx.doi.org/10.2525/ecb.50.63.

Marcelis, L.F.M., Broekhuijsen, A.G.M., 2006. Quantification of the growth response to light quantity of greenhouse grown crops. pp. 97–104.

Marrou, H., Wery, J., Dufour, L., Dupraz, C., 2013. Productivity and radiation use efficiency of lettuces grown in the partial shade of photovoltaic panels. Eur. J. Agron. 44, 54–66. http://dx.doi.org/10.1016/j.eja.2012.08.003.

Mizuno, T., Amaki, W., Watanabe, H., 2011. Effects of monochromatic light irradiation by LED on the growth and anthocyanin contents in leaves of cabbage seedlings. Acta Hortic. 907, 179–184. http://dx.doi.org/10.17660/ActaHortic.2011.907.25.

Mohamed, E.A.H., Yam, M.F., Ang, L.F., Mohamed, A.J., Asmawi, M.Z., 2013. Antidiabetic properties and mechanism of action of orthosiphon stamineus benth bioactive sub-fraction in Streptozotocin-induced diabetic rats. JAMS J. Acupunct. Meridian Stud. 6, 31–40. http://dx.doi.org/10.1016/j.jams.2013.01.005.

Moreira, J., Klein-Júnior, L.C., Filho, V.C., Buzzi, F.D.C., 2013. Anti-hyperalgesic activity of corilagin, a tannin isolated from Phyllanthus niruri L. (Euphorbiaceae). J. Ethnopharmacol. 146, 318–323. http://dx.doi.org/10.1016/j.jep.2012.12.052.

Natephra, W., Yabuki, N., Fukuda, T., 2018. Optimizing the evaluation of building envelope design for thermal performance using a BIM-based overall thermal transfer value calculation. Build. Environ. 136, 128–145. http://dx.doi.org/10.1016/j.buildenv.2018.03.032.

Nielsen, V., 2018. What effect does red light have on plants? http://ursalighting.com/effect-red-light-plants/ (Accessed 22 November 2019).

Northern, M., Seminar, C., 2016. OTTV in UBBL & how OTTV applies to building envelope.

NREL Transforming ENERGY, 2018. High-efficiency crystalline photovoltaics. https://www.nrel.gov/pv/high-efficiency-crystalline-photovoltaics.html. (Accessed 27 September 2019).

Oraee, M., Luther, M., 2015. The next step in energy rating : the international ETTV method vs. BCA section-J Glazing Calculator the next step in energy rating : the international ETTV method vs. BCA section - J Glazing Calculator.

Othman, N.F., Ya'acob, M.E., Abdul-Rahim, A.S., Mohd. Shahwahid, O., Hizam, H., Ramlan, M.F., 2016. Integration of solar dryer technologies in high value herbal crops production for Malaysia: Pathway for a sustainable future. Int. Food Res. J. 23, S51–S55.

Othman, N.F., Ya'acob, M.E., Abdul-Rahim, A.S., Shahwahid Othman, M., Radzi, M.A.M., Hizam, H., Wang, Y.D., Ya'Acob, A.M., Jaafar, H.Z.E., 2015. Embracing new agriculture commodity through integration of Java Tea as high value Herbal crops in solar PV farms. J. Clean. Prod. 91, 71–77. http://dx.doi.org/10.1016/j.jclepro.2014.12.044.

Rahman, M.M., Hasanuzzaman, M., Rahim, N.A., 2015. Effects of various parameters on PV-module power and efficiency. Energy Convers. Manag. 103, 348–358. http://dx.doi.org/10.1016/j.enconman.2015.06.067.

Ringsmuth, A.K., Landsberg, M.J., Hankamer, B., 2016. Can photosynthesis enable a global transition from fossil fuels to solar fuels, to mitigate climate change and fuel-supply limitations? Renew. Sustain. Energy Rev. 62, 134–163. http://dx.doi.org/10.1016/j.rser.2016.04.016.

Roslan, N., Ya, M.E., Jamaludin, D., Iskandar, A.N., Othman, M.H., 2019. Dye Sensitized Solar Cell Field Performance in Tropical Climatic Condition: A Case Study. 020001, pp. 1–6. http://dx.doi.org/10.1063/1.5118009.

Roslan, N., Ya'acob, M.E., Radzi, M.A.M., Hashimoto, Y., Jamaludin, D., Chen, G., 2018. Dye sensitized solar cell (DSSC) greenhouse shading: New insights for solar radiation manipulation. Renew. Sustain. Energy Rev. 92, 171–186. http://dx.doi.org/10.1016/j.rser.2018.04.095.

Schettini, E., Scarascia, G., Vox, G., 2011. Radiometric properties of photoselective and photoluminescent greenhouse plastic films and their effects on peach and cherry tree growth. http://dx.doi.org/10.1080/14620316.2011.11512729.

Seghier, T.E., Lim, Y.W., Ahmad, M.H., Samuel, W.O., 2017. Building envelope thermal performance assessment using visual programming and Bim, based on ETTV requirement of Green Mark and GreenRE. Int. J. Built Environ. Sustain. 4, 227–235. http://dx.doi.org/10.11113/ijbes.v4.n3.216.

Selvaraj, P., Baig, H., Mallick, T.K., Siviter, J., Montecucco, A., Li, W., Paul, M., Sweet, T., Gao, M., Knox, A.R., Sundaram, S., 2018. Enhancing the efficiency of transparent dye-sensitized solar cells using concentrated light. Sol. Energy Mater. Sol. Cells 175, 29–34. http://dx.doi.org/10.1016/j.solmat.2017.10.006.

Sharma, K., Sharma, V., Sharma, S.S., 2018. Dye-sensitized solar cells: Fundamentals and current status. Nanoscale Res. Lett. 13, http://dx.doi.org/10.1186/s11671-018-2760-6.

Siddiqui, M.U., Arif, A.F.M., 2013. Electrical, thermal and structural performance of a cooled PV module: Transient analysis using a multiphysics model. Appl. Energy 112, 300–312. http://dx.doi.org/10.1016/j.apenergy.2013.06.030.

Singhpoo, C., Punnucharoenwong, N., Benjapiyaporn, C., 2015. Study of the effect of temperature differences on the overall thermal transfer value of buildings. Energy Proced. 79, 348–353. http://dx.doi.org/10.1016/j.egypro.2015.11.501.

Skandalos, N., Karamanis, D., 2015. PV glazing technologies. Renew. Sustain. Energy Rev. 49, 306–322. http://dx.doi.org/10.1016/j.rser.2015.04.145.

Taki, M., Rohani, A., Rahmati-joneidabad, M., 2018. Solar thermal simulation and applications in greenhouse. Inf. Process. Agric. 5, 83–113. http://dx.doi.org/10.1016/j.inpa.2017.10.003.

Upton, R., David, B., Gafner, S., Glasl, S., 2019. Botanical ingredient identification and quality assessment: strengths and limitations of analytical techniques. Phytochem. Rev. http://dx.doi.org/10.1007/s11101-019-09625-z, 0123456789.

Vijayalaxmi, J., 2010. Concept of overall thermal transfer value (OTTV) in design of building envelope to achieve energy efficiency. Int. J. Therm. Environ. Eng. 1, 75–80. http://dx.doi.org/10.5383/ijtee.01.02.003.

Wikipedia, 2019. Botanical drug. https://en.wikipedia.org/wiki/Botanical_drug. (Accessed 17 December 2019).

Wong, W.S., Chan, H.W., 2012. Energy and Use of Energy: Calculation and Application of OTTV and U-Value. Hong Kong Inst. Archit..

Yang, E.J., Song, K.S., 2014. Andrographolide, a major component of andrographis paniculata leaves, has the neuroprotective effects on glutamate-induced HT22 cell death. J. Funct. Foods 9, 162–172. http://dx.doi.org/10.1016/j.jff.2014.04.023.

Yano, A., Cossu, M., 2019. Energy sustainable greenhouse crop cultivation using photovoltaic technologies. Renew. Sustain. Energy Rev. 109, 116–137. http://dx.doi.org/10.1016/j.rser.2019.04.026.

Zanoli, P., Zavatti, M., Montanari, C., Baraldi, M., 2009. Influence of Eurycoma longifolia on the copulatory activity of sexually sluggish and impotent male rats. J. Ethnopharmacol. 126, 308–313. http://dx.doi.org/10.1016/j.jep.2009.08.021.

Zingre, K.T., Wan, M.P., Yang, X., 2015. A new RTTV (roof thermal transfer value) calculation method for cool roofs. Energy 81, 222–232. http://dx.doi.org/10.1016/j.energy.2014.12.030.